




Pulmonary clearance kinetics and extrapulmonary translocation of seven titanium dioxide nano- and submicron materials following intratracheal administration in rats

Naohide Shinohara, Yutaka Oshima, Toshio Kobayashi, Nobuya Imatanaka, Makoto Nakai, Takayuki Ichinose, Takeshi Sasaki, Kenji Kawaguchi, Guihua Zhang & Masashi Gamo

To cite this article: Naohide Shinohara, Yutaka Oshima, Toshio Kobayashi, Nobuya Imatanaka, Makoto Nakai, Takayuki Ichinose, Takeshi Sasaki, Kenji Kawaguchi, Guihua Zhang & Masashi Gamo (2015) Pulmonary clearance kinetics and extrapulmonary translocation of seven titanium dioxide nano- and submicron materials following intratracheal administration in rats, *Nanotoxicology*, 9:8, 1050-1058, DOI: [10.3109/17435390.2015.1015644](https://doi.org/10.3109/17435390.2015.1015644)

To link to this article: <http://dx.doi.org/10.3109/17435390.2015.1015644>

 View supplementary material 

 Published online: 04 May 2015.

 Submit your article to this journal 

 Article views: 50

 View related articles 

 View Crossmark data 

ORIGINAL ARTICLE

Pulmonary clearance kinetics and extrapulmonary translocation of seven titanium dioxide nano- and submicron materials following intratracheal administration in rats

Naohide Shinohara¹, Yutaka Oshima², Toshio Kobayashi², Nobuya Imatanaka³, Makoto Nakai², Takayuki Ichinose⁴, Takeshi Sasaki⁵, Kenji Kawaguchi⁵, Guihua Zhang¹, and Masashi Gamo¹

¹Research Institute of Science for Safety and Sustainability, National Institute of Advanced Industrial Science and Technology (AIST), Tsukuba, Ibaraki, Japan, ²Chemicals Evaluation and Research Institute (CERI), Hita, Oita, Japan, ³Chemicals Evaluation and Research Institute (CERI), Bunkyo, Tokyo, Japan, ⁴Toray Research Center, Inc., Otsu, Shiga, Japan, and ⁵Nanosystem Research Institute, National Institute of Advanced Industrial Science and Technology (AIST), Tsukuba, Ibaraki, Japan

Abstract

We evaluated and compared the pulmonary clearance kinetics and extrapulmonary translocations of seven titanium dioxide (TiO₂) nano- and submicron particles with different characteristics, including size, shape and surface coating. Varying doses of TiO₂ nano- and submicron particles dispersed in 0.2% disodium phosphate solution were intratracheally administered to male F344 rats. The rats were euthanized under anesthesia for 3, 28 and 91 days after administration. Ti levels in pulmonary and various extrapulmonary organs were determined using inductively coupled plasma-sector field mass spectrometry (ICP-SFMS). The lungs, including bronchoalveolar lavage fluid (BALF), contained 55–89% of the administered TiO₂ dose at 3 days after administration. The pulmonary clearance rate constants, estimated using a one-compartment model, were higher after administration of 0.375–2.0 mg/kg body weight (bw) (0.016–0.020/day) than after administration of 3.0–6.0 mg/kg bw (0.0073–0.013/day) for six uncoated TiO₂. In contrast, the clearance rate constant was 0.011, 0.0046 and 0.00018/day following administration of 0.67, 2.0 and 6.0 mg/kg bw TiO₂ nanoparticle with Al(OH)₃ coating, respectively. Translocation of TiO₂ from the lungs to the thoracic lymph nodes increased in a time- and dose-dependent manner. Furthermore, the translocation of TiO₂ from the lungs to the thoracic lymph nodes after 91 days was higher when Al(OH)₃ coated TiO₂ was administered (0.93–6.4%), as compared to uncoated TiO₂ (0.016–1.8%). Slight liver translocation was observed (<0.11%), although there was no clear trend related to dose or elapsed time. No significant translocation was observed in other organs including the kidney, spleen and brain.

Keywords

Distribution, liver, lymph node, rate constant, toxicokinetics

History

Received 9 December 2014
Revised 2 February 2015
Accepted 2 February 2015
Published online 4 May 2015

Introduction

Worldwide concern regarding the toxicity of nanomaterials has increased, owing to the lack of information regarding their potential risks for workers and the general population. Thus, the toxicity of nanomaterials has been investigated internationally. Titanium dioxide (TiO₂) nanoparticles (particle size <100 nm) are one of the most common industrial nanomaterials, and are used in a variety of applications, including sunscreen, cosmetics and photo catalysis. Since TiO₂ is water-insoluble and inert, it is generally regarded as having low toxicity in humans, and is even used as an additive in food products. A wide variety of TiO₂ nanoparticles have been developed and applied, which have different physicochemical properties.

In general, chemical substances with the same chemical formula have the same toxicity, regardless of manufacturer and processing. In contrast, nanomaterials have different toxicities

depending on their physicochemical characteristics, including size, shape and surface coating, even if the nanomaterials have the same chemical formula. Studies have been performed comparing toxicities between nanomaterials having different physicochemical properties (Borm et al., 2006). However, differences in nanomaterial toxicokinetics remain unclear.

To evaluate the toxicity of TiO₂ nanoparticles, toxicokinetic data are beneficial. It is well-established that pulmonary clearance is inhibited when high particle dose are administered, also known as overload (Morrow, 1992). Thus, it is important to understand the effect of nanoparticle dose on pulmonary clearance when determining the lung toxicity.

After the respiratory system is exposed to nanoparticles, both lung retention and translocation from the lung to extrapulmonary organs are of relevance. Following inhalation or intratracheal administration of TiO₂ nanoparticles, Ti has been detected in the lungs and lung-associated lymph nodes (Bermudez et al., 2004; Ma-Hock et al., 2009; Oyabu et al., 2013; Sager et al., 2008; Shinohara et al. 2014b; van Ravenzwaay et al., 2009). Ti was also detected in the liver using a highly sensitive analytical method; however, the amount translocated was low (Shinohara et al., 2014b).

Correspondence: Dr Naohide Shinohara, Research Center for Chemical Risk Management, National Institute of Advanced Industrial Science and Technology (AIST), Tsukuba, Ibaraki 305-8569, Japan. Tel: +81-29-861-8415. Fax: +81-29-861-8030. E-mail: n-shinohara@aist.go.jp

Table 1. Characteristics of TiO₂ particles used in the present study.

Material	Shape ^a	Primary particle size ^a (nm)	Surface coating ^a	Crystalline form ^a	Surface area ^a (m ² /g)	Z-average diameter of agglomerate in the suspension ^b (nm)	ζ-Potential of agglomerate in the suspension ^c (mV)
P25	Spherical	21	No	Rutile 20/ Anatase 80	50 ± 15	113–140	−43.7
MT-150AW	Spindle-shape	Long axis: 28.8 short axis: 7.6	No	Rutile	100–120	91–94	−37.9
AMT-100	Spherical	6	No	Anatase	250–300	189–199	−22.4
MP-100	Spherical	1000	No	Rutile	6	333–400	−47.2
FTL-100	Needle-like	Length: 1680 diameter: 130	No	Rutile	12.0	–	−51.0
TTOS-3 without coating	Spindle-shape	Long axis: 50–100 short axis: 10–20	No	Rutile	102	69–79	−41.3
TTOS-3 with coating	Spindle-shape	Long axis: 50–100 short axis: 10–20	Al(OH) ₃	Rutile	93.0	235–299	−40.2

^aThese data are described using the data from the catalog or obtained from the manufacturer.

^bThese data ranges were determined for all of the concentrations in the present study.

^cThese data were determined for 2.0 mg/mL in the present study.

In this study, we intratracheally administered seven TiO₂ nano- or submicron materials to rats and evaluated how their physicochemical properties affected pulmonary clearance kinetics and extrapulmonary translocation. We determined the TiO₂ burden in the lungs, bronchoalveolar lavage fluid (BALF), trachea, thoracic lymph nodes, liver, spleen, kidneys and brain using an accurate inductively coupled plasma double-focusing sector field mass spectrometry (ICP-SFMS; double-focusing ICP-MS) method. The pulmonary clearance rate constants, which were estimated using a one-compartment model, were compared among the different doses and among the different TiO₂ characteristics.

Materials and methods

TiO₂ particles used in the study

Seven TiO₂ particles with different characteristics including primary particle sizes (6 nm–1 μm), surface areas (6–300 m²/g), agglomerate sizes (69–400 nm), shapes (spherical, spindle-shape, needle-like), crystalline forms (rutile and anatase), and surface coatings (no coating and Al(OH)₃ coating), were used in the present study. The TiO₂ particles were AEROSIL[®] P25 (Nippon Aerosil Co. Ltd., Tokyo, Japan), MT-150AW, AMT-100, MP-100 (Tayca Co. Ltd., Osaka, Japan), FTL-100, TTOS-3 without coating, and TTOS-3 with Al(OH)₃ coating (Ishihara Sangyo Kaisha, Ltd., Osaka, Japan). The characteristics of these particles, which were described in catalog, obtained from manufacturer, or measured, are shown in Table 1. The organ burden of P25 nanoparticles was determined 1, 3, 7, 28, 91 and 182 days after the administration, and the clearance kinetics were evaluated using the six time points obtained in a previous study (Shinohara et al., 2014b). We determined the organ burden for the other six TiO₂ nano- and submicron particles in the present study. We evaluated the kinetics of seven TiO₂ nano- and submicron particles using the organ burden data for three time points (3, 28 and 91 days after administration) in the present study.

Preparation of TiO₂ suspension

TiO₂ particles (2 g) were sonicated in 50 mL of 0.2% disodium phosphate solution (DSP; food additive grade, Wako Pure Chemical Industries, Ltd., Tokyo, Japan) for 1–3 h in an ultrasonic bath (5510J-MT; Branson Ultrasonics Co., Danbury, CT), followed by centrifugation at 20–1000 g for 5–40 min at 20 °C

(CF16RXII and T15A41; Hitachi Koki Co., Ltd., Tokyo, Japan) as shown in Table S1. The supernatant (40 mL) was collected as a stock suspension. To adjust the concentration of the administered suspension, the concentration of the stock suspension was determined by a usual weight analysis, where the weight loss of the suspension was measured by the balance (AUW220D; Shimadzu Co., Kyoto, Japan) after drying at 200 °C in a thermostatic chamber (ON-300S; Azone Co., Osaka, Japan). Suspensions of 0.375, 0.75, 1.5, 3.0 and 6.0 mg/mL for P25 and 0.67, 2.0 and 6.0 mg/mL for the other TiO₂ particles were prepared by diluting the stock suspension with 0.2% DSP. The size of the TiO₂ agglomerates in the suspension was determined by the method of dynamic light scattering (DLS) (Zetasizer nano-ZS; Malvern Instruments Ltd., Worcestershire, UK) for all of the concentrations. The ζ-potential of the TiO₂ agglomerates in 2.0 mg/mL suspension was also determined using DLS.

Experimental procedure

All the animals were treated in accordance with the guidelines for animal experiments in our laboratory, which referred to the guidelines of the Ministry of the Environment, Ministry of Health, Labour and Welfare, Ministry of Agriculture, Forestry and Fisheries, and Ministry of Education, Culture, Sports, Science and Technology. The present experiment was approved by the Animal Care and Use Committee, Chemicals Evaluation and Research Institute, and by the Institutional Animal Care and Use Committee of the National Institute of Advanced Industrial Science and Technology.

Male F344/DuCrIj rats were obtained from Charles River Laboratories Japan, Inc. (Kanagawa, Japan). The animals were 12 weeks old with a mean body weight of 251 ± 12 g (212–282 g) at the start of the study, which was the adequate body size for intratracheal administration. The mean body weight did not differ among different TiO₂ treated groups (Table S2). Rats were anesthetized by isoflurane inhalation and intratracheally administered the negative control or TiO₂ particles (0.67, 2.0, and 6.0 mg/kg body weight [bw]) in 0.2% DSP at 1 mL/kg body weight using a MicroSprayer[®] Aerosolizer (Model IA-1B-R for Rat; Penn-Century, Inc., Wyndmoor, PA). Assuming the exposure concentrations to be 0.47, 1.4 and 4.2 mg/m³ for 13 weeks (8 h/day, 5 days/week), the lung burden was estimated to be 0.67, 2.0 and 6.0 mg/kg bw, using a deposition fraction of 0.15 and a clearance rate constant of 0.015/day. The concentration was within the range of the TiO₂ particles' concentration in

occupational environment (0.18–18 mg/m³) (Ichihara et al., 2008; Witschger et al., 2010).

Five rats in each group were euthanized and dissected on days 3, 28 and 91 post-TiO₂ administration. The animals were euthanized by exsanguination from the abdominal aorta under intraperitoneal pentobarbital anesthesia (50 mg/kg bw). Thereafter, the trachea was cannulated with a disposable feeding needle, which was then tied in place. The lungs were lavaged with 7 mL of physiological saline freely flowing from 30 cm above the rat. This fluid was collected in a tube placed 30 cm below the rat. The lavage was performed twice and >90% of the lavage fluid was recovered. After BALF sampling, the trachea, lungs, right and left posterior mediastinal lymph nodes, parathymic lymph nodes, liver, kidneys, spleen and brain of each animal were dissected, rinsed with saline and weighed.

Analysis

The Ti content in the lungs after BALF sampling, BALF, trachea, right and left mediastinal lymph nodes, parathymic lymph nodes, and liver of all animals were analyzed. The Ti content in the kidney, spleen and brain of the negative control and the highest dose groups was also analyzed, as well as the Ti content in the stock suspensions.

The lungs after BALF, kidney and spleen samples were homogenized with 2 mL of ultrapure water (Milli-Q Advantage A10 Ultrapure Water Purification System, Merck Millipore, Billerica, MA), and the liver was homogenized with 10 mL of ultrapure water. An electric homogenizer (PT10-35 Kinematica AG, NS-50 and NS-52; Microtec Co. Ltd., Chiba, Japan) was used. The resulting homogenates were stored at –30 °C until analysis.

All samples were treated with acid prior to determining the Ti and Al levels, using nitric acid (HNO₃; 68%), and hydrofluoric acid (HF; 38%) as shown in Table S3. HF was used for samples from rats that administered MP-100 and FTL-100, because the Ti recovery efficiency from the spiked organ tissue samples was >90%. In contrast, without HF, the Ti recovery efficiency from the spiked organ tissue samples were 49 ± 4.9% and 27 ± 3.8%, respectively. For the other five TiO₂ materials, the Ti recovery efficiency from the spiked organ tissue samples was >85%. For TTOS-3 with Al(OH)₃ coating, Al recovery efficiency from the spiked organ tissue samples was >94%. All acids used in the study were ultrapure grade reagents (TAMAPURE-AA-100, Tama Chemicals Co., Ltd., Kanagawa, Japan). The acidified samples were placed in a 7-mL perfluoroalkylvinylether (PFA) vessel, which was inserted into a 100 mL digestion vessel in a microwave sample preparation instrument (ETHOS 1; Milestone Srl, Italy or Speedwave 4; Berghof, Germany). The mixtures were heated to 180 °C for 20 min. After cooling to 40 °C, the acid-treated samples, with the exception of the TiO₂ suspensions, were diluted to 5 mL or 10 mL (as shown in Table S3) with ultrapure water (PURELAB Option-R 7 and PURELAB Flex UV, Veolia Water Solutions and Technologies, Antony, France). Samples from the acid-treated TiO₂ suspensions were heated on a hot plate for approximately 2 h until white fuming sulfuric acid was generated. After cooling, the solution was diluted to 50 mL with 10% HNO₃.

The Ti and Al content of the samples was determined by ICP-SFMS (ELEMENT 2/ELEMENT XR; Thermo Fisher Scientific Inc., Bremen, Germany), and the Ti and Al content of the administered TiO₂ suspensions was determined by ICP atomic emission spectrometry (ICP-AES; SPS4000, Hitachi High-Tech Science Co., Tokyo, Japan). Analytical conditions for ICP-SFMS were same as previously described (Shinohara et al., 2014a). In the present study, ⁴⁹Ti (mass: 48.9479) and ²⁷Al (mass: 26.9815) were analyzed. Linearity of the calibration curves for ⁴⁹Ti and

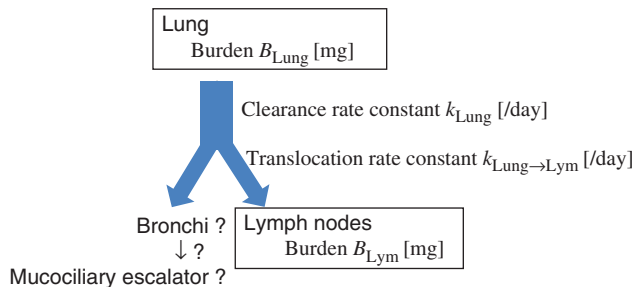


Figure 1. One-compartment models for the clearance of TiO₂ nano- and submicron particles. This model is expressed using a first-order decay equation with rate constant k .

²⁷Al using ICP-SFMS were good between 0 and 20 ng/mL of standard solution (0, 0.01, 0.05, 0.1, 1, 5, 10 and 20 ng/mL; $R^2 > 0.999$). The instrumental limit of quantification was 0.02 ng/mL based on the 10 σ of signals for blank samples ($N = 10$). Based on the operation blank for the organ tissue samples, the limit of quantification was 20, 10 and 2 ng/g for lungs, trachea and the other organ tissues, 1 ng/mL for BALF and 0.5 ng for lymph nodes.

TiO₂ clearance analysis using decay model fitting

To express the pulmonary clearance and translocation to lymph nodes, the model shown in Figure 1 was used. Although a two-compartment model was better fit to evaluate the pulmonary clearance of particles (Shinohara et al., 2014b), a one-compartment model was used in the present study to evaluate the pulmonary clearance because the number of time points (three points) were not enough to use a two-compartment model. It was presumed that the fraction which did not reach the alveolar region was cleared via conducting airway within 3 days of administration. The one-compartment model can be represented by a one-step clearance rate constant, as shown in Equation (1), where B_{Lung} was the TiO₂ lung burden; D was the amount of TiO₂ administered dose (μ g); t was the time elapsed after administration (days); r was the fraction that reached the alveolar region following TiO₂ administration; and k_{Lung} was the clearance rate constant for the clearance (/day).

$$\frac{dB_{Lung}}{dt} = -k_{Lung}B_{Lung} \quad (t = 0: B_{Lung} = rD) \quad (1)$$

Curve fitting was conducted using the least squares approach, as shown in Equation (2), where $RMSE$ is root mean square error, $B_{Lung_measured}$ is the measured lung burden, and $B_{Lung_estimated}$ is the estimated lung burden, obtained using the Solver tool in Excel 2010 (Microsoft Co., Redmond, WA).

$$RMSE = \sqrt{\frac{\sum (\ln B_{Lung_measured} - \ln B_{Lung_estimated})^2}{n}} \quad (2)$$

TiO₂ translocation rate coefficients to the thoracic lymph nodes

Assuming that TiO₂ is cleared from the lungs to the thoracic lymph nodes depending on the lung burden, and that the burden in the thoracic lymph nodes is not cleared (Figure 1), the rate constants for the translocation of TiO₂ from the lungs to thoracic lymph nodes were estimated by Equation (3), using the given lung burden estimated by a one-compartment model.

$$\frac{dB_{Lym}}{dt} = k_{Lung \rightarrow Lym}B_{Lung} \quad (t = 0: B_{Lym} = 0) \quad (3)$$

where B_{Lym} was the total TiO₂ burden in thoracic lymph nodes (right and left mediastinal lymph nodes, and parathymic lymph nodes; μg); B_{Lung} was the TiO₂ lung burden estimated as described above (μg); and $k_{\text{Lung} \rightarrow \text{Lym}}$ was the translocation rate constant from lungs to thoracic lymph nodes (/day).

The least squares method (Equation (4)) was used for the estimation.

$$RMSE = \sqrt{\frac{\sum (\text{Ln}B_{\text{Lym_measured}} - \text{Ln}B_{\text{Lym_estimated}})^2}{n}} \quad (4)$$

where $RMSE$ is root mean square error, $B_{\text{Lym_measured}}$ is the measured TiO₂ burden in the thoracic lymph nodes, and $B_{\text{Lym_estimated}}$ is the estimated TiO₂ burden in the thoracic lymph nodes under the condition that $k_{\text{Lung} \rightarrow \text{Lym}}$ does not exceed k_{Lung} .

Statistical analysis

A two-way repeated analysis of variance (ANOVA) with the Scheffe test was employed to compare the difference in TiO₂ organ tissue concentrations among the study groups after an F -test using SPSS 20.0 (IBM Co., Armonk, NY). The data from solvent administered rats in the P25-treated experimental group were used as a negative control for all tests. For values below the quantification limit, 1/2 of the quantification limit was used for the calculation of the mean and standard deviation. In addition, since the administered doses were different depending on the body weight, the organ burdens were shown as normalized values, where the organ burden was divided by the body weight when TiO₂ particles were administered.

Results

Characteristics of administered nano- and submicron materials

The mean sizes of the nano- and submicron materials in suspension, as measured by DLS, were 69–400 nm (Table 1). The materials were agglomerated in suspension, because the sizes of all the materials except MP-100 were larger than the sizes described in the catalog and/or obtained from the manufacturer. The primary particle sizes of the bulk MP-100 powder, as determined by scanning electron microscopy (SEM), were smaller than the sizes described in the catalog or obtained from the manufacturer, suggesting that they could also be agglomerated in suspension. All suspensions were stably dispersed within -22 and -51 mV of the ζ potentials. No sedimentation was observed in the suspensions during administration.

TiO₂ and Al(OH)₃ concentrations in suspension

The TiO₂ concentrations (TiO₂ and Al(OH)₃ concentrations for TTOS-3 with coating) in the diluted suspensions, as determined by ICP-AES, were >90% of the concentration estimated by weight measurement, accounting for dilution. However, the recovery efficiencies were slightly low for TTOS-3 with and without Al(OH)₃ coating for 0.67 mg/kg bw (0.72 and 0.78 mg/mL; 82 and 84% recovery, respectively). The ratios of Ti/Al (measured value) and TiO₂/Al(OH)₃ (calculated value) in the suspensions of TTOS-3 with Al(OH)₃ coating were 92%/7.5%–92%/8.2% (Table S4) and 88%/12%–87%/13%, respectively.

Organ TiO₂ burdens

TiO₂ burdens per initial body weight at the time of administration in the lungs after BALF sampling and in the BALF were significantly higher ($p < 0.01$) than those of the control group from day 3 to 91 (Figure 2(A); Table S5 (A), (B)). The burdens

were normalized (divided) by the initial body weight at the time of administration and expressed as the unit “mg/kg bw (mg/organ/kg bw)” because the administered doses were set depending on the initial body weight at administration. Thus, the initial burden varied among rats in the same group, whereas the initial burden per initial body weight was same among rats in the same group. For reference, the TiO₂ burdens per organ tissue weight (unit: mg/g tissue) are also shown in Table S6. TiO₂ burdens in the lungs after BALF sampling and BALF depended on the dose administered and decreased over time. Three days after administration, although the lung burdens varied between 55 and 89% of the administered TiO₂ dose, there were no clear trends among doses and among materials. The lung burden three days after the administration represented the burden in the alveolar region, and the rest of the administered dose could be trapped on the bronchi and bronchiole and cleared by the rapid mucociliary clearance from the conduction airways. For the particles without coating, 91 days after administration, the lungs retained 9.0–18% of the administered TiO₂ for doses of 0.375–2.0 mg/kg bw and 21–37% for doses of 3.0–6.0 mg/kg bw. For the TTOS-3 nanoparticles coated with Al(OH)₃, 91 days after administration, the lungs retained 28, 47 and 61% of the TiO₂ administered for doses of 0.67, 2.0 and 6.0 mg/kg bw, respectively. The ratios of Ti/Al in the lungs, including BALF, did not differ from the suspensions, and were not altered over time and among doses (Table S4). The relative percentage of the TiO₂ burden in BALF to the total lung burden of TiO₂ decreased over time, with values of 2.6–12%, 0.86–9.6% and 0.88–11% at 3, 28 and 91 days after administration, respectively (Table 2). Although it was not statistically significant, higher fractions in the BALF were observed at lower doses and with longer observation periods.

TiO₂ burdens per the initial body weight at the time of administration in the total thoracic lymph nodes (total burden in the right and left posterior mediastinal lymph nodes, and parathymic lymph nodes) are shown in Figure 2(B) and Table S5(D). The TiO₂ burdens in most of the thoracic lymph nodes were significantly higher in the groups dosed with TiO₂ particles, as compared to the control group. The TiO₂ burden in the thoracic lymph nodes increased over time, and was higher in the high-dose groups than in the low-dose groups from day 3 to 91. The percent burden detected in the thoracic lymph nodes relative to the administered TiO₂ doses was 0.012–0.068%, 0.022–0.18% and 0.092–0.30% for doses of 0.375–0.75, 1.5–3.0 and 6.0 mg/kg bw 3 days after administration, respectively. Ninety-one days after administration, the percent burden of TiO₂ in the thoracic lymph nodes was 0.016–0.93%, 0.071–3.3% and 0.54–6.4% for doses of 0.375–0.75, 1.5–3.0 and 6.0 mg/kg bw, respectively. Although TiO₂ burden per initial body weight at the time of administration in the thoracic lymph nodes was not different among the seven TiO₂ particles, including TTOS-3 with Al(OH)₃ coating, at three days after the administration, the percent of TiO₂ burden in the thoracic lymph nodes among administered doses was higher for TTOS-3 with Al(OH)₃ coating than the six uncoated TiO₂ particles 91 days after administration. The percent burden in the lymph nodes on day 91 were 0.016–0.47%, 0.071–0.84% and 0.54–1.8% at doses of 0.67, 2.0 and 6.0 mg/kg bw for the uncoated particles. In contrast, the percentage of TTOS-3 with Al(OH)₃ in the lymph nodes 91 days after administration was 0.93, 3.3 and 6.4% at doses of 0.67, 2.0 and 6.0 mg/kg bw. In most rats, a higher TiO₂ burden was detected in the right and left mediastinal lymph nodes than in the parathymic lymph node (Table S7).

In evaluations using TTOS-3 with Al(OH)₃ coating, the ratio of Ti/Al in the thoracic lymph nodes was not different from those in suspension at 28 and 91 days after administration, although the ratios of Ti/Al in the thoracic lymph nodes was slightly lower three days after administration due to background (Table S4).

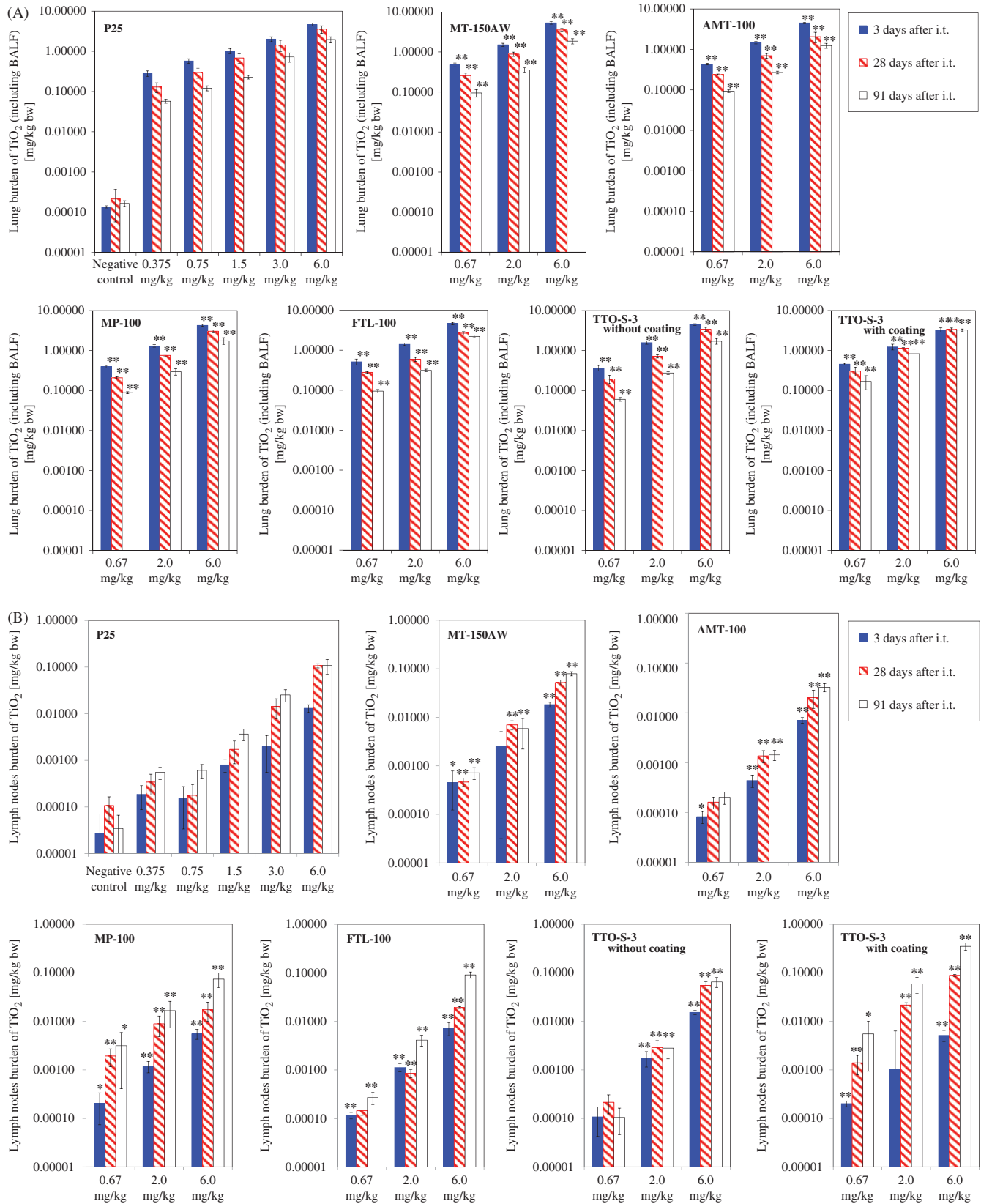


Figure 2. TiO₂ burden per initial body weight at the time of administration in the lungs, including BALF (A), in the total thoracic lymph nodes (right mediastinal lymph node and left and right mediastinal lymph nodes) (B), and in the liver (C) following intratracheal TiO₂ administration. The columns and error bars indicate the mean and standard deviation, respectively. Asterisks indicate statistically significant differences, compared with the control group (**p < 0.01, *p < 0.05). Samples with TiO₂ levels below the quantification limit were assigned values corresponding to half the quantification limit.

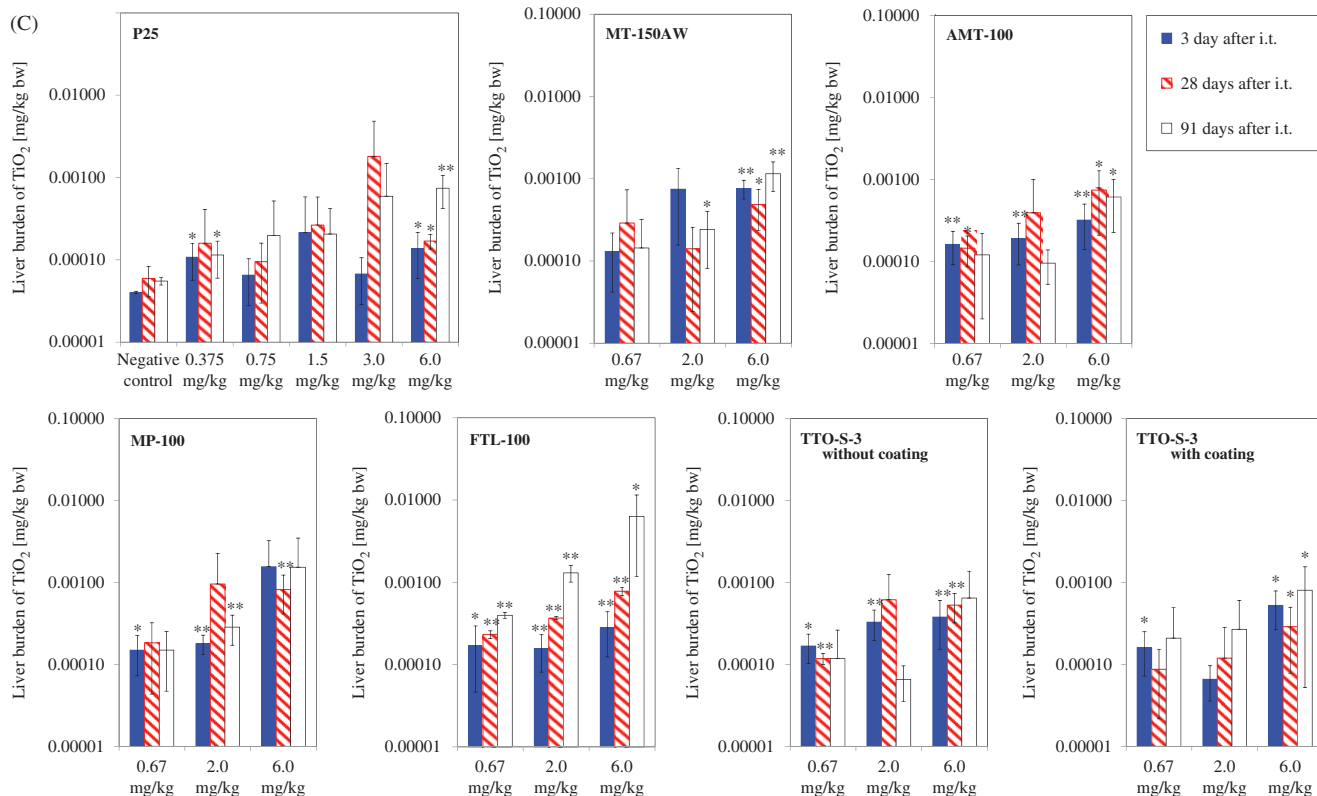


Figure 2. Continued.

Table 2. TiO₂ in BALF per total lung burden.

Material/Dose (mg/kg bw)	BALF/(lung + BALF) of TiO ₂		
	3 Days	28 Days	91 Days
P25			
0.375	5.6% ± 0.92%	5.3% ± 0.73%	5.0% ± 0.81%
0.75	5.8% ± 1.5%	5.2% ± 0.66%	4.9% ± 0.97%
1.5	5.2% ± 0.96%	4.5% ± 0.80%	5.3% ± 0.45%
3.0	5.0% ± 1.5%	3.5% ± 1.2%	3.0% ± 0.78%
6.0	4.3% ± 0.90%	1.6% ± 0.98%	3.4% ± 1.8%
MT 150AW			
0.67	12% ± 2.4%	9.4% ± 0.40%	6.4% ± 2.1%
2.0	10% ± 8.6%	8.5% ± 2.4%	11% ± 8.0%
6.0	4.5% ± 1.1%	4.6% ± 0.73%	3.3% ± 0.32%
AMT 100			
0.67	8.9% ± 0.66%	5.5% ± 0.62%	4.7% ± 0.91%
2.0	6.6% ± 1.6%	6.0% ± 1.5%	4.6% ± 0.50%
6.0	5.4% ± 0.78%	5.2% ± 0.60%	3.2% ± 0.32%
MP 100			
0.67	10% ± 1.4%	6.3% ± 0.94%	5.2% ± 1.1%
2.0	7.4% ± 2.2%	4.1% ± 1.9%	4.8% ± 1.2%
6.0	5.2% ± 2.1%	3.1% ± 0.30%	2.0% ± 0.39%
FTL 100			
0.67	9.7% ± 0.74%	9.2% ± 0.94%	5.4% ± 0.91%
2.0	7.2% ± 1.9%	8.5% ± 2.6%	3.4% ± 0.42%
6.0	4.0% ± 0.71%	3.8% ± 0.89%	0.88% ± 0.25%
TTOS-3 without coating			
0.67	6.0% ± 1.5%	4.6% ± 2.4%	8.7% ± 1.6%
2.0	3.8% ± 0.55%	4.8% ± 1.1%	5.9% ± 1.7%
6.0	2.7% ± 0.95%	2.7% ± 0.85%	3.3% ± 0.45%
TTOS-3 with Al(OH)₃ coating			
0.67	2.6% ± 0.43%	3.4% ± 0.80%	2.9% ± 1.5%
2.0	4.2% ± 1.3%	1.9% ± 1.0%	2.6% ± 1.0%
6.0	3.4% ± 0.84%	0.86% ± 0.38%	2.3% ± 1.4%

TiO₂ burdens per initial body weight at the time of administration in the liver are shown in Figure 2(C) and Table S5(E). The liver TiO₂ burdens were higher than those in the negative control group although some were not statistically significant. However, no clear trend was observed between different doses and times, with the exception of FTL-100, where 0.0022–0.037% of the administered dose was detected in the liver 91 days after administration. For FTL-100, the burden in the liver was increased at higher doses and over time. Three days after administration, 0.025 ± 0.019%, 0.0078 ± 0.0037% and 0.0047 ± 0.0026% burden was observed following doses of 0.67, 2.0 and 6.0 mg/kg bw, respectively. Ninety-one days after administration, 0.059 ± 0.0051%, 0.065 ± 0.015% and 0.11 ± 0.086% burden was observed following doses of 0.67, 2.0 and 6.0 mg/kg bw, respectively. No significant differences were observed in kidney, spleen and brain TiO₂ levels between TiO₂ treatment groups at the highest dose and control animals.

TiO₂ clearance analysis using one-compartment models

The clearance rate constants estimated by the one-compartment model are shown in Table 3. The pulmonary clearance rate constants, k_{Lung} , were higher at TiO₂ doses of 0.375–2.0 mg/kg bw (0.016–0.020/day) than TiO₂ doses of 3.0–6.0 mg/kg bw (0.0073–0.013/day) for the six uncoated TiO₂ particles. The clearance rate constants for TTOS-3 with Al(OH)₃ coating also decreased dose-dependently, and were lower than the other six TiO₂ nano- and submicron particles, with values of 0.011, 0.0046 and 0.00018/day at doses of 0.67, 2.0 and 6.0 mg/kg bw, respectively (Figure 3A).

TiO₂ translocation rate constants to the thoracic lymph nodes

The rate constants of translocation to the thoracic lymph nodes, $k_{Lung \rightarrow Lym}$, increased depending on the dose of the nano- and

submicron particles, with a $k_{\text{Lung} \rightarrow \text{Lym}}$ of 0.000023–0.00014/day for doses of 0.375–0.75 mg/kg bw, 0.000049–0.00042/day for doses of 1.5–3.0 mg/kg bw, and 0.00028–0.00072/day for doses of 3.0–6.0 mg/kg bw for the six TiO₂ nano- and submicron-sized agglomerates/aggregates. In contrast, a dose-dependent trend was not observed for submicron-sized MP-100, which has the largest size, with values of 0.00019, 0.00029 and 0.00028/day at doses of 0.67, 2.0 and 6.0 mg/kg bw, respectively (Figure 3B).

Table 3. Pulmonary clearance rate constants and initial fraction of the administered TiO₂ that reached the alveolar region estimated using the lung and BALF burden data using a one-compartment model.

Material/Dose (mg/kg bw)	Clearance rate constants k_{Lung} [1/day]	Initial fraction reaching the alveolar region r [%]	Root mean square error (RMSE)
P25			
0.375	0.017	68	0.15
0.75	0.017	74	0.10
1.5	0.017	73	0.010
3.0	0.011	68	0.022
6.0	0.0097	79	0.010
MT-150AW			
0.67	0.018	70	0.071
2.0	0.016	75	0.059
6.0	0.012	88	0.50
AMT-100			
0.67	0.017	63	0.074
2.0	0.018	69	0.12
6.0	0.013	65	0.19
MP-100			
0.67	0.016	57	0.097
2.0	0.017	65	0.058
6.0	0.0098	70	0.42
FTL-100			
0.67	0.019	77	0.061
2.0	0.016	61	0.20
6.0	0.0073	68	0.16
TTOS-3 without coating			
0.67	0.020	55	0.058
2.0	0.019	73	0.13
6.0	0.011	77	0.0012
TTOS-3 with Al(OH)₃ coating			
0.67	0.011	77	0.054
2.0	0.0046	73	0.013
6.0	0.00018	63	0.011

Discussion

In the present study, the primary particle size (6 nm to a few hundred nanometers), surface area (6–300 m²/g), agglomerate size (69 nm–400 nm), shape (spherical, spindle-shape, needle-like), and crystalline form (rutile and anatase) rarely affected the pulmonary clearance and toxicokinetics of TiO₂ particles. Al(OH)₃ coating decreased the pulmonary clearance.

The clearance of TTOS-3 coated with Al(OH)₃ was slow (0.011/day), even at the lowest dose of 0.67 mg/kg bw, and further decreased to 0.00018/day at 6.0 mg/kg bw. Although the six uncoated TiO₂ materials had different sizes, shapes and crystalline forms, the pulmonary clearance rate constants did not differ. The primary and agglomerate sizes of TTOS-3 coated with Al(OH)₃ were in the range of the six uncoated TiO₂ particles, and some materials had the same shape and crystalline form as TTOS-3 with Al(OH)₃ coating. Thus, the Al(OH)₃ coating was likely the reason for slow clearance.

Regarding the relationship between size and clearance, in previous studies (Ferin et al., 1992; Oberdörster et al., 1994), ultrafine TiO₂ particles (inhalation exposure, primary size: 20 nm, agglomerate size: 710 nm, peak lung burden: 5.2 mg/lung) were cleared slower from the lungs than fine TiO₂ particles (inhalation exposure, primary size: 250 nm, agglomerate size: 780 nm, peak lung burden: 6.6 mg/lung). In contrast, the clearance rates were not different among different sizes of TiO₂ particles in the present study (intratracheal administration, primary size: 6 nm to a few hundred nanometers, agglomerate size: 69–400 nm, peak lung burden: 0.09–1.5 mg/lung). The lung burden and exposure method were different between the studies. Thus, if the lung burden was higher in the present study, differences in clearance may have been observed among different particle sizes.

Regarding the relationship between shape and clearance, a previous study showed that belt-shaped TiO₂ nanomaterials (7 μm of length) were cleared more slowly than two types of spherical TiO₂ particles after intratracheal administration (size ~24 nm and ~28 nm, dose 20, 70, 200 μg/rat) (Silva et al., 2013). Further, belt-shaped TiO₂ (length: 6–12 μm, dose: 30 μg/mice) showed slower clearance than spherical TiO₂ particles after intratracheal administration (size: 70–190 nm, dose: 30 μg/mice) (Porter et al., 2013). In contrast, the clearance rate constants did not differ among the different shaped TiO₂ nano- and submicron particles in the present study. The difference could be due to the length of the needle-like TiO₂ materials in the present study, which were shorter than those of the belt-shaped TiO₂ materials in the previous studies (6–12 μm).

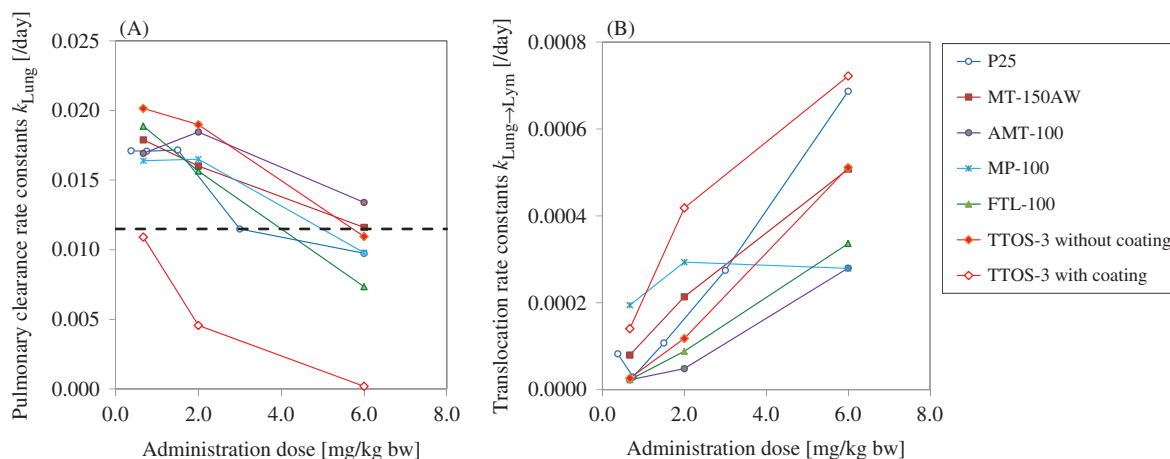


Figure 3. Dose-dependent pulmonary clearance rate constants (A) and translocation rate constants from the lungs to the thoracic lymph nodes (B). Broken line in (A) shows the 2-month half-life (0.0115/day).

In a previous study, regarding the relationship between crystalline form and clearance, (Ismagilov et al., 2012), it was reported that the amorphous TiO₂ and anatase TiO₂ can penetrate into cells, whereas rutile TiO₂ cannot penetrate cells. This was because amorphous TiO₂ and anatase TiO₂ are likely to agglomerate into smaller particles (amorphous TiO₂: 200 nm, anatase TiO₂: 40–90 nm, rutile TiO₂: 1200 nm). In contrast, rutile TiO₂ does not always agglomerate into larger particles, and the clearance rates were not different among the different crystalline forms of TiO₂ in the present study. In the present study, the agglomerate size of anatase TiO₂ and anatase/rutile TiO₂ agglomerates were larger than some rutile TiO₂ agglomerates and smaller than the other rutile TiO₂ agglomerates. Therefore, the difference in clearance between different crystalline forms as shown by Ismagilov et al. (2012) could not be due to the crystalline form, but due to the size of agglomerate.

The clearance rate constants were decreased depending on the administered doses of TiO₂. In particular, the clearance rate constants were significantly decreased (0.0073–0.013 /day) at 3.0–6.0 mg/kg bw for the six uncoated TiO₂ particles as shown in Figure 3. Since the body weights (250 g) and lung weights (1.5 g) were approximately equal, the clearance delay of the lung burden was 0.5–1.0 mg/g lung. This threshold was similar to previous inhalation studies, which showed that, at lung burdens of 1 mg/g lung or greater, there is prolonged retention of particles, known as overload (Morrow, 1992; Pauluhn, 2009). Nevertheless, there could be differences between the inhalation exposure and intratracheal administration: regional burdens may be higher after intratracheal administration than after inhalation exposure, since inhalation exposure showed more uniform distribution than intratracheal administration (Brain et al., 1976; Leong et al., 1998).

Translocation to the thoracic lymph nodes increased over time for each TiO₂ particles after intratracheal administration, as well as after inhalation (Bermudez et al., 2004; van Ravenzwaay et al., 2009) and intratracheal administration in the previous studies (Shinohara et al., 2014b). Since translocation of TiO₂ nanoparticles to the thoracic lymph nodes was not observed in the previous intravenous administration tests (Fabian et al., 2008; Shinohara et al., 2014a), it is possible that TiO₂ materials translocate from lungs to lymph nodes via the interstitium, rather than the blood.

Since nearly all clearance from the lungs occurred via translocation to the thoracic lymph nodes ($k_{\text{Lung}} = k_{\text{Lung} \rightarrow \text{Lym}}$) at 6.0 mg/kg bw TTOS-3 coated with Al(OH)₃, the other pulmonary clearance pathways were thought to be almost completely inhibited. In contrast, for the other six TiO₂ nanoparticles, only 2.1–7.9% of pulmonary clearance occurred via the thoracic lymph nodes. Based on these results, the translocation of macrophages ingesting Al(OH)₃-coated TiO₂ nanoparticles to terminal bronchioles could be inhibited. Therefore, Al(OH)₃ coated TiO₂ nanoparticles themselves, and not ingested in macrophages, may translocate to the thoracic lymph nodes via interstitium.

Since the Ti/Al ratio in the thoracic lymph nodes was not different from the Ti/Al ratio in suspension and the lungs (although the deviations were large; Table S4), Al(OH)₃ and/or Al ion did not behave independently from core TiO₂ nanoparticles. It was reported in previous studies that Al(OH)₃ coating rarely dissolved or was absorbed. Al(OH)₃ was not dissolved from TiO₂ particles after a 3-hour acidic treatment (0.2% HCl), which is a representative of gastrointestinal fluid (Fisichella et al., 2012a,b). Al(OH)₃ used as an acid suppressant was rarely absorbed after ingestion (~1%) (Berthon, 2002).

Since more than 90% of intravenously injected P25 TiO₂ nanoparticles were accumulated in the liver 6 h post-injection (Shinohara et al., 2014b), it was thought that most TiO₂

nanoparticles would accumulate in the liver if TiO₂ nanoparticles translocated from the lungs to the blood. Although this trend was not clear, the data suggested that a slight translocation occurs from lungs to liver. However, the nanoparticle with the highest translocation, FTL-100, exhibited a maximum accumulation in the liver at 0.11% of the administered dose. The TiO₂ burden in the kidneys, spleen and brain were not different between the TiO₂ treated groups and the negative control group. Thus, the translocation of TiO₂ nanoparticles from the lungs to the blood was low.

Conclusion

In the present study, the tissue distribution and clearance of seven TiO₂ nanoparticles, which have different characteristics, such as size, shape and surface coating, were determined 3, 28 and 91 days after intratracheal administration in rats. The pulmonary clearance rate constants were estimated using a one-compartment model, and were found to be higher at low doses of TiO₂. In addition, the pulmonary clearance rate constants were much higher for TiO₂ nanoparticles with Al(OH)₃ coating than the six uncoated TiO₂ nanoparticles. The translocation rate coefficients to the thoracic lymph nodes increased depending on the nanoparticle dose. The translocation rate constants to the thoracic lymph nodes were not different among the seven TiO₂ nanoparticles. Significant translocation to the extrapulmonary organs, such as kidney, spleen and brain were not observed.

Declaration of interest

This work is part of the research program “Development of innovative methodology for safety assessment of industrial nanomaterials” supported by the Ministry of Economy, Trade and Industry (METI) of Japan.

References

- Bermudez E, Mangum JB, Wong BA, Asgharian B, Hext PM, Warheit DB, Everitt JI. 2004. Pulmonary responses of mice, rats, and hamsters to subchronic inhalation of ultrafine titanium dioxide particles. *Toxicol Sci* 77:347–57.
- Berthon G. 2002. Aluminium speciation in relation to aluminium bioavailability, metabolism and toxicity. *Coord Chem Rev* 228:319–41.
- Born PJA, Robbins D, Haubold S, Kuhlbusch T, Fissan H, Donaldson K, et al. 2006. The potential risks of nanomaterials: a review carried out for ECETOC. *Part Fibre Toxicol* 3:11.
- Brain JD, Knudson DE, Sorokin SP, Davis MA. 1976. Pulmonary distribution of particles given by intratracheal instillation or by aerosol inhalation. *Environ Res* 11:13–33.
- Fabian E, Landsiedel R, Ma-Hock L, Wiench K, Wohlleben W, van Ravenzwaay B. 2008. Tissue distribution and toxicity of intravenously administered titanium dioxide nanoparticles in rats. *Arch Toxicol* 82: 151–7.
- Ferin J, Oberdörster G, Penney DP. 1992. Pulmonary retention of ultrafine and fine particles in rats. *Am J Resp Cell Mol Biol* 6:535–42.
- Fisichella M, Berenguer F, Steinmetz G, Auffan M, Rose J, Prat O. 2012a. Intestinal toxicity evaluation of TiO₂ degraded surface-treated nanoparticles: a combined physico-chemical and toxicogenomics approach in caco-2 cells. *Part Fibre Toxicol* 9:18.
- Fisichella M, Berenguer F, Steinmetz G, Auffan M, Rose J, Prat O. 2012b. Reply to comment on Fisichella et al., “Intestinal toxicity evaluation of TiO₂ degraded surface-treated nanoparticles: a combined physico-chemical and toxicogenomics approach in Caco-2 cells” by Faust et al. *Part Fibre Toxicol* 9:39.
- Ichihara G, Li W, Kobayashi T, Ding X, Fujitani Y, Liu Y, et al. (2008). Assessment of exposure and health status in workers handling titanium dioxide. International Conference on Safe Production and Use of Nanomaterials. NANOSAFE 2008, Nov 3–7, Minatec, Greboble, France.
- Ismagilov ZR, Shikina NV, Mazurkova NA, Tsikoza LT, Tuzikov FV, Ushakov VA, et al. (2012). Synthesis of nanoscale TiO₂ and study of

- the effect of their crystal structure on single cell response. *Scientific World J* 2012: Article ID 498345.
- Leong BKJ, Coombs JK, Sabaitis CP, Rop DA, Aaron CS. 1998. Quantitative morphometric analysis of pulmonary deposition of aerosol particles inhaled via intratracheal nebulization, intratracheal instillation or nose-only inhalation in rats. *J Appl Toxicol* 18:149–60.
- Ma-Hock L, Burkhardt S, Strauss V, Gamer A, Wiench K, van Ravenzwaay B, Landsiedel R. 2009. Development of a short-term inhalation test in the rat using nano-titanium dioxide as a model substance. *Inhal Toxicol* 21:102–18.
- Morrow PE. 1992. Dust overloading of the lungs - update and appraisal. *Toxicol Appl Pharmacol* 113:1–12.
- Oberdörster G, Ferin J, Lehnert BE. 1994. Correlation between particle-size, in-vivo particle persistence, and lung injury. *Environ Health Perspect* 102:173–9.
- Oyabu T, Morimoto Y, Hirohashi M, Horie M, Kambara T, Lee BW, et al. 2013. Dose-dependent pulmonary response of well-dispersed titanium dioxide nanoparticles following intratracheal instillation. *J Nanopart Res* 15:1600.
- Pauluhn J. 2009. Pulmonary toxicity and fate of agglomerated 10 and 40 nm aluminum oxyhydroxides following 4-week inhalation exposure of rats: toxic effects are determined by agglomerated, not primary particle size. *Toxicol Sci* 109:152–67.
- Porter DW, Wu N, Hubbs AF, Mercer RR, Funk K, Meng F, et al. 2013. Differential mouse pulmonary dose and time course responses to titanium dioxide nanospheres and nanobelts. *Toxicol Sci* 131:179–93.
- Sager TM, Kommineni C, Castranova V. 2008. Pulmonary response to intratracheal instillation of ultrafine versus fine titanium dioxide: role of particle surface area. *Part Fibre Toxicol* 5:17.
- Shinohara N, Danno N, Ichinose T, Sasaki T, Fukui H, Honda K, Gamo M. 2014a. Tissue distribution and clearance of intravenously administered titanium dioxide (TiO₂) nanoparticles. *Nanotoxicology* 8:132–41.
- Shinohara N, Oshima Y, Kobayashi T, Imatanaka N, Nakai M, Ichinose T, et al. 2014b. Dose-dependent clearance kinetics of intratracheally administered titanium dioxide nanoparticles in rat lung. *Toxicology* 325:1–11.
- Silva RM, Teesy C, Franzi L, Weir A, Westerhoff P, Evans JE, Pinkerton KE. 2013. Biological response to nano-scale titanium dioxide (TiO₂): role of particle dose, shape, and retention. *J Toxicol Environ Heal A* 76:953–72.
- van Ravenzwaay B, Landsiedel R, Fabian E, Burkhardt S, Strauss V, Ma-Hock L. 2009. Comparing fate and effects of three particles of different surface properties: nano-TiO₂, pigmentary TiO₂ and quartz. *Toxicol Lett* 186:152–9.
- Witschger O, Wrobel R, Bianchi B, Bau S. 2010. Potential for exposure during bagging operations in a plant that produces both pigment grade TiO₂ and nano-TiO₂ as powders. *International Conference on Safe Production and Use of Nanomaterials. Nanosafe 2010*, Nov 16–18, Minatéc, Greboble, France.

Supplementary material available online

Supplementary Tables S1–S7.